



**HAL**  
open science

## **Cell-penetrating peptides with intracellular actin-remodeling activity in malignant fibroblasts.**

Diane Delaroche, François-Xavier Cantrelle, Frédéric Subra, Carine van Heijenoort, Eric Guittet, Chen-Yu Jiao, Laurent Blanchoin, Gérard Chassaing, Solange Lavielle, Christian Auclair, et al.

► **To cite this version:**

Diane Delaroche, François-Xavier Cantrelle, Frédéric Subra, Carine van Heijenoort, Eric Guittet, et al.. Cell-penetrating peptides with intracellular actin-remodeling activity in malignant fibroblasts.. Journal of Biological Chemistry, 2010, 285 (10), pp.7712-21. 10.1074/jbc.M109.045872 . hal-00464266

**HAL Id: hal-00464266**

**<https://hal.science/hal-00464266>**

Submitted on 31 May 2020

**HAL** is a multi-disciplinary open access archive for the deposit and dissemination of scientific research documents, whether they are published or not. The documents may come from teaching and research institutions in France or abroad, or from public or private research centers.

L'archive ouverte pluridisciplinaire **HAL**, est destinée au dépôt et à la diffusion de documents scientifiques de niveau recherche, publiés ou non, émanant des établissements d'enseignement et de recherche français ou étrangers, des laboratoires publics ou privés.

Copyright

# Cell-penetrating Peptides with Intracellular Actin-remodeling Activity in Malignant Fibroblasts<sup>\*S</sup>

Received for publication, July 17, 2009, and in revised form, December 22, 2009. Published, JBC Papers in Press, December 27, 2009, DOI 10.1074/jbc.M109.045872

Diane Delaroche<sup>‡S</sup>, François-Xavier Cantrelle<sup>S</sup>, Frédéric Subra<sup>¶</sup>, Carine Van Heijenoort<sup>S</sup>, Eric Guittet<sup>S</sup>, Chen-Yu Jiao<sup>‡</sup>, Laurent Blanchoin<sup>||</sup>, Gérard Chassaing<sup>‡</sup>, Solange Lavielle<sup>‡</sup>, Christian Auclair<sup>¶</sup>, and Sandrine Sagan<sup>‡1</sup>

From the <sup>‡</sup>Laboratoire des Biomolécules, Université Pierre et Marie Curie (UPMC), CNRS, 4 place Jussieu, F-75005 Paris, the <sup>S</sup>Institut de Chimie des Substances Naturelles, Laboratoire de Chimie et Biologie Structurales, CNRS, F-91198 Gif-sur-Yvette Cedex, the <sup>¶</sup>Laboratoire de Biotechnologies et de Pharmacologie Génétique Appliquée, Ecole Normale Supérieure Cachan, CNRS, F-94235 Cachan Cedex, and the <sup>||</sup>Institut de Recherches en Technologies et Sciences pour le Vivant/Laboratoire de Physiologie Cellulaire Végétale, Commissariat à l'Énergie Atomique Grenoble, F-38054 Grenoble Cedex 9, France

Cell-penetrating peptides can cross cell membranes and are commonly seen as biologically inert molecules. However, we found that some cell-penetrating peptides could remodel actin cytoskeleton in oncogene-transformed NIH3T3/EWS-Fli cells. These cells have profound actin disorganization related to their tumoral transformation. These arginine- and/or tryptophan-rich peptides could cross cell membrane and induce stress fiber formation in these malignant cells, whereas they had no perceptible effect in non-tumoral fibroblasts. In addition, motility (migration speed, random motility coefficient, wound healing) of the tumor cells could be decreased by the cell-permeant peptides. Although the peptides differently influenced actin polymerization *in vitro*, they could directly bind monomeric actin as determined by NMR and calorimetry studies. Therefore, cell-penetrating peptides might interact with intracellular protein partners, such as actin. In addition, the fact that they could reverse the tumoral phenotype is of interest for therapeutic purposes.

Since the initial evidence that antennapedia homeobox (1–3) protein can cross cell membranes came to light, numerous peptides with similar internalization properties have been described (4). These cell-penetrating peptides are more or less amphipathic peptides generally rich in lysyl and arginyl residues. It is now well accepted that these peptides can enter cells through direct translocation and endocytosis pathways and thus that they can end up into the cytosol of the cell (5, 6). In addition, cell-penetrating peptides are widely used as conjugates to vehiculate inside bioactive molecules of the cell such as peptides, proteins, or nucleic acids (7, 8). Contrasting with the biologically active homeoproteins (9), cell-penetrating peptides are commonly accepted as inert molecules devoid of biological activity, although cytotoxicity problems may occur, generally over high  $\mu\text{M}$  concentrations (10).

In a completely different context, some peptides rich in basic amino acids (Lys and Arg), such as those derived from

myristoylated alanine-rich C kinase substrate (MARCKS)<sup>2</sup> or MARCKS-related protein, have been shown to interact with actin *in vitro* (11). In addition, polyamine and MARCKS peptides have been reported to induce actin polymerization (12–15). Polycations and basic polypeptides or proteins were more generally described as actin-bundling factors at physiologic concentrations (16–18). In addition, polymerization of cellular actin is a dynamic process controlled by numerous actin-binding proteins (19, 20). These proteins have common domains of interaction, characterized in structural studies to be generally organized in short more or less amphipathic helices (21, 22). These helices generally bind to a hydrophobic cleft between subdomains 1 and 3 of actin, as for thymosin  $\beta 4$  (23, 24).

In this context, we have screened some cell-penetrating peptide analogues (25) (penetratin, (R/L)16, (R/W)16, (R/W)9, and R9), which present basic amino acids or sequences of charged/hydrophobic residues with the potential to form amphipathic helices, for their ability to influence actin dynamics in a cell-free assay based on fluorescence anisotropy (26). In this actin polymerization assay, only (R/W)16, (R/W)9, and R9 were found active. Therefore, these latter peptides were further tested for their capability to interact with actin *in vitro* and in 3T3-EF fibroblasts lacking zyxin focal adhesion points and stress fibers (27).

## EXPERIMENTAL PROCEDURES

**Peptides**—The following peptides were obtained by solid-phase synthesis (*t*-butoxycarbonyl strategy) as described (28): trifluoroacetyl( $\alpha,\alpha$ -diethyl)Gly-Lys(Nebiotin)-(D)Lys-Cys-RRWRRRWR-NH<sub>2</sub> ((R/W)9), trifluoroacetyl( $\alpha,\alpha$ -diethyl)Gly-Lys(Nebiotin)-(D)Lys-Cys-(D)Arg-(D)Arg-(D)Trp-(D)Trp-(D)Arg-(D)Arg-(D)Trp-(D)Arg-(D)Arg-NH<sub>2</sub> ((D)(R/W)9), biotinyl-Apa-RRWRRRWR-NH<sub>2</sub> ((R/W)16), and biotinyl-Apa-RRRRRRRR-NH<sub>2</sub> (Bapa-R9). Thymosin  $\beta 4$  (T $\beta 4$ ) and actin were prepared as described earlier (29).

<sup>2</sup> The abbreviations used are: MARCKS, myristoylated alanine-rich C kinase substrate; T $\beta 4$ , thymosin  $\beta 4$ ; ITC, isothermal titration calorimetry; TRITC, tetramethylrhodamine isothiocyanate; BSA, bovine serum albumin; (R/W)9, trifluoroacetyl( $\alpha,\alpha$ -diethyl)Gly-Lys(Nebiotin)-(D)Lys-Cys-RRWRRRWR-NH<sub>2</sub>; (D)(R/W)9, trifluoroacetyl( $\alpha,\alpha$ -diethyl)Gly-Lys(Nebiotin)-(D)Lys-Cys-(D)Arg-(D)Arg-(D)Trp-(D)Trp-(D)Arg-(D)Arg-(D)Trp-(D)Arg-(D)Arg-NH<sub>2</sub>; (R/W)16, biotinyl-Apa-RRWRRRWR-NH<sub>2</sub>; R9, RRRRRRRRR-NH<sub>2</sub>; (R/L)-16, biotinyl-Apa-RRLRLLRLLRRLRR-NH<sub>2</sub> penetratin, biotinyl-Apa-RQIKIWFQNRMRKWK-NH<sub>2</sub>.

<sup>\*</sup> This work was supported by Agence Nationale pour la Recherche Grant 05-BLAN0269.

<sup>S</sup> The on-line version of this article (available at <http://www.jbc.org>) contains supplemental Fig. S1.

<sup>1</sup> To whom correspondence should be addressed. Tel.: 33-1-44-27-55-09; Fax: 33-1-44-27-71-50; E-mail: sandrine.sagan@upmc.fr.

**Cell Culture**—NIH 3T3 and NIH 3T3 EF cells were cultured in Dulbecco's modified Eagle's medium supplemented with 10% newborn calf serum (Invitrogen), penicillin (100,000 IU/liter), and streptomycin (100,000 IU/liter) (PAA Laboratories) and selected with 25  $\mu\text{g}/\text{ml}$  puromycin (Sigma).

**Isothermal Titration Calorimetry (ITC)**—ITC measurements were performed on a VP-ITC system (MicroCal). Peptides solutions at 100  $\mu\text{M}$  in G buffer were titrated in 10- $\mu\text{l}$  injections into 1.45 ml of a 10  $\mu\text{M}$  actin solution in G buffer (50 mM Tris, pH 7.6, 0.1 mM  $\text{CaCl}_2$ , 0.2 mM ATP, 1 mM dithiothreitol, 1%  $\text{NaN}_3$ ) at 25 °C. The duration of the injections was 20 s with an interval of 4 min between two injections. Data were fitted to a one-site binding model using the MicroCal Origin software to determine the  $K_d$  values of peptide-actin association.

**NMR Experiments**—NMR experiments were performed on a Bruker Avance 600-MHz spectrometer equipped with a 5-mm TXI cryoprobe. 1.45 mM (R/W)16 and (R/W)9 peptide stock solutions were prepared in 90%  $\text{H}_2\text{O}$ , 10%  $\text{D}_2\text{O}$  G buffer. NMR samples of complexes between G actin and peptides were prepared by mixing 500  $\mu\text{l}$  of 50  $\mu\text{M}$  G-actin in G buffer with increasing amounts of peptide stock solution. It should be noted that G-actin polymerization in G buffer is negligible at this concentration. The binding was followed by one-dimensional  $^1\text{H}$  experiments at 298 K. Water resonance was suppressed using a WATERGATE sequence. Experiments were repeated at least three times independently. Competition experiments were done between a 1:1 complex T $\beta$ 4-G-actin in which T $\beta$ 4 was uniformly  $^{15}\text{N}$ -labeled and (R/W)16. The T $\beta$ 4-G-actin complex was prepared by mixing 550  $\mu\text{l}$  of 50  $\mu\text{M}$  G-actin in G buffer with 1.5 mg of [ $^{15}\text{N}$ ]T $\beta$ 4 (29). A small excess of T $\beta$ 4 was added to avoid polymerization of G-actin. (R/W)16 was added into this sample at different ratios (0; 0.2; 0.4; 0.6; 0.8; 1.0; 1.2). The titration was followed through the observation of the  $^1\text{H}$ - $^{15}\text{N}$  resonances of T $\beta$ 4 in a  $^1\text{H}$ - $^{15}\text{N}$  heteronuclear single quantum correlation experiment performed at 298 K. The spectra were transformed with the software NMRPipe (30) and analyzed with SPARKY (46).

**Actin-Pyrene Polymerization Assays**—Pyrene-labeled and unlabeled actin monomers (3  $\mu\text{M}$ ) were mixed to obtain 10% pyrene-actin in G buffer. The polymerization reaction was started by the addition of 10 $\times$  KMEI (500 mM KCl, 10 mM  $\text{MgCl}_2$ , 10 mM EGTA and 100 mM imidazole-HCl, pH 7) in the absence or the presence of the peptides at the indicated concentration. Kinetics of polymerization was obtained by measurement of the fluorescence signal increase related to actin-pyrene incorporation into actin polymers (31).

**Morphological Study by Fluorescent Immunostaining**—Cells (10<sup>5</sup> cells/well) were seeded on the glass coverslips coated with fibronectin (10  $\mu\text{g}/\text{ml}$ ) in 2 ml of Dulbecco's modified Eagle's medium with 10% newborn calf serum. After peptide incubation for 2 or 18 h, cells were washed twice with phosphate-buffered saline, fixed for 15 min with 3% paraformaldehyde, and permeabilized for 5 min with 0.4% Triton X-100 before incubation with 3% bovine serum albumin in phosphate-buffered saline. Anti-zyxin antibody (Synaptic Systems) (1/200) was incubated with cells for 30 min at room temperature. Cells were then incubated with phalloidin-fluorescein isothiocyanate (1/1000) (Sigma) and

a donkey anti-mouse IgG antibody conjugated to TRITC (1/100) (Jackson ImmunoResearch) for 30 min at room temperature. Cells were finally incubated with 4',6-diamidino-2-phenylindole (1.5  $\mu\text{g}/\text{ml}$ ) (Pierce) in phosphate-buffered saline for 15 min in the dark at room temperature. Coverslips were mounted in Fluoromount for observation with a Nikon Eclipse TE2000-S, objective  $\times 60$  PLANFLUOR.

**Cell Motility by Video Microscopy**—Cells were seeded in 8-well Lab-Tek chamber slides (Nunc) on a glass coverslip (10<sup>4</sup> cells/well) in 400  $\mu\text{l}$  of Dulbecco's modified Eagle's medium/10% newborn calf serum. Cells were incubated with the peptide in hermetic chamber at 37 °C in a humidified 5%  $\text{CO}_2$  atmosphere (Leica). Video recordings of EF cell migration were done on glass coverslips in parallel: 3T3 cells, EF cells, EF cells in the presence of 5 or 10  $\mu\text{M}$  (R/W)16. Phase contrast photographs were taken every 4 min for 18 h with a high resolution camera (Leica). The movements of the cells were analyzed with MetaMorph software (Universal Imaging, Downingtown, PA), allowing the reconstitution of each cell track and the measurement of the motility parameters.

**Anchorage-independent Growth Assay**—Cells were seeded (500 cells/dish) in complete culture medium supplemented with 1% methylcellulose (Methocel MC4000, Sigma) in triplicate into 35-mm dishes. Peptides were added every 3 days to cells incubated at 37 °C in a humidified 5%  $\text{CO}_2$  atmosphere. After 3 weeks, pictures of each dish were taken, and clones with a diameter  $> 120$   $\mu\text{m}$  were counted.

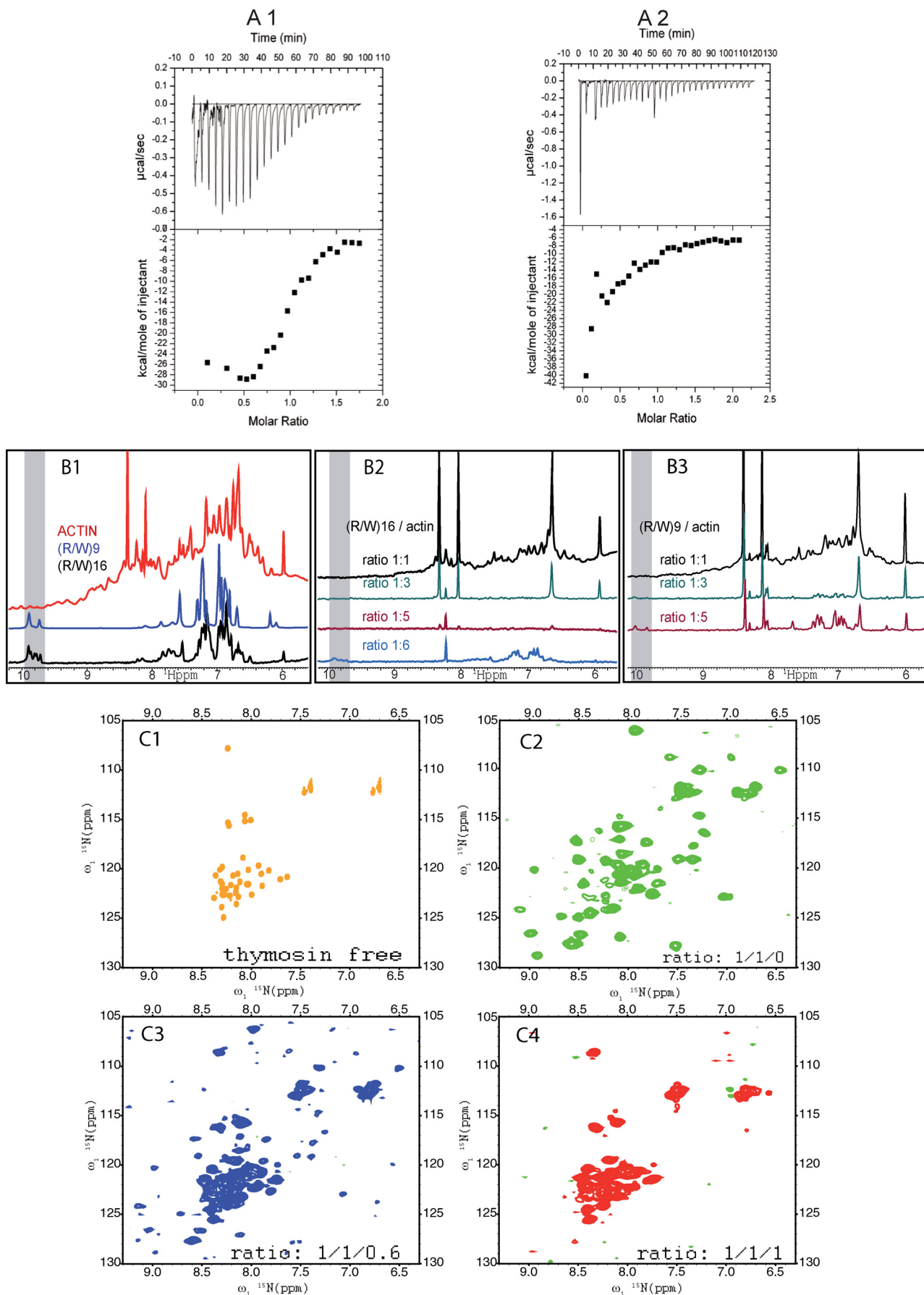
**Wound Healing Assay**—Fibroblasts were grown nearly to confluence in the absence or the presence of 10  $\mu\text{M}$  peptide. A linear wound was then made with a sterile 100- $\mu\text{l}$  plastic pipette tip. Cells were additionally grown for 24 h before contrast phase microscopy observation.

## RESULTS

**(R/W)16, (R/W)9, and R9 Interact Directly with G-actin**—The putative interaction of (R/W)16, (R/W)9, and R9 with G-actin was first examined by ITC. All three peptides were found to interact with G-actin but with different affinity (Fig. 1, A1). The affinity for G-actin of (R/W)16 was higher than the one of (R/W)9 (Fig. 1, A2) or R9 (not shown), with  $K_d$  values of 0.4 and  $\sim 10$   $\mu\text{M}$ , respectively. The enantiomeric form of (R/W)9, containing all D-amino acids, did not interact with G-actin (not shown).

The interaction of (R/W)16 and (R/W)9 with actin was also examined by NMR spectroscopy (Fig. 1B). Fig. 1, B1, presents the signal of free G-actin (in red), free (R/W)9 (in blue), and free (R/W)16 (in black). The G-actin spectrum is best described as a large envelope of broad signals with a limited number of narrower resonances possibly corresponding to more dynamic regions of the protein and/or minor low molecular weight impurities in the preparation. This broad spectrum is expected for a 42-kDa folded protein. At the opposite, narrow lines and weak spectral dispersion spectra are detected for (R/W)9 and (R/W)16, which agree with small unfolded peptides without G-actin. The signals around 10 ppm correspond to the chemical shift of side chain protons of tryptophan. We use it to follow the behavior of the peptides in the presence of G-actin. No resonances characteristic of the free peptide were detected at

# Cell-penetrating Peptide-induced Stress Fiber Formation



the early stages of the titration of a 50  $\mu\text{M}$  G-actin solution with (R/W)9 and (R/W)16 (Fig. 1, B2 and B3), whereas the  $^1\text{H}$  resonances of G-actin progressively disappeared upon the addition of up to 1 eq of one or the other peptide (Fig. 1, B2 for (R/W)16 and Fig. 1, B3 for (R/W)9). First, the disappearance of G-actin resonances upon peptide addition indicates the formation of large particles that can no longer be detected by liquid state NMR. The simultaneous disappearance of the peptide resonances confirmed a direct *in vitro* interaction of (R/W)16 and (R/W)9 with G-actin.  $^1\text{H}$  resonances characteristic of the free peptides and corresponding to a concentration of about 1 eq of peptide arise upon the addition of the 6th and 3rd eq of (R/W)16 and (R/W)9, respectively (Fig. 1, B1 and B2). (R/W)9 thus exhibits a lower affinity and/or a lower interaction stoichiometry than (R/W)16 for actin. Finally, the binding competition of (R/W)16 with T $\beta$ 4, a known actin sequestering peptide, was evaluated by NMR  $^1\text{H}$ - $^{15}\text{N}$  correlation spectra of  $^{15}\text{N}$ -labeled T $\beta$ 4. The large dispersion of amide resonances in the bound form of  $^{15}\text{N}$ -labeled T $\beta$ 4 is typical of a fully structured protein, whereas at the opposite, the free-form spectrum displays poor dispersion, indicating an unfolded peptide. The  $^{15}\text{N}$  and  $^1\text{H}$  resonances of T $\beta$ 4 bound to G-actin were gradually displaced toward the free form upon the addition of (R/W)16 (Fig. 1, C and D). Considering that the dissociation constant of thymosin  $\beta$ 4 for G-actin is around 0.76  $\mu\text{M}$  (19), the ability of (R/W)16 to completely displace at a stoichiometry of 1:1:1 this actin-binding protein from G-actin is wholly compatible with the 0.4  $\mu\text{M}$  dissociation constant obtained from ITC measurements. The cooperative global unbinding of thymosin  $\beta$ 4 upon titration by (R/W)16 indicates that the binding site of (R/W)16 covers a fraction of the extended binding site of thymosin  $\beta$ 4 that is crucial for the binding of the whole protein, that (R/W)16 modifies the structure of G-actin in such a way that it disrupts the binding of thymosin  $\beta$ 4, or that (R/W)16 favors actin aggregation, thus impeding thymosin  $\beta$ 4 binding. In any case, the results clearly show a direct interaction between (R/W)16 and G-actin.

**(R/W)16 Speeds Up the Rate of Actin Polymerization**—Fluorescence assays with 10% pyrene-labeled actin (31) were used to evaluate whether these peptides could directly affect actin polymerization dynamics. Up to 10  $\mu\text{M}$  of the (R/W)9 and R9 peptides had no significant effect in these polymerization assays (not shown), whereas (R/W)16 could speed up the rate of actin polymerization (Fig. 2A). Indeed, the slope ( $\Delta\text{fluorescence}/\Delta t$ ), determined at half-polymerization, was increased in a concentration-dependent manner from 0.97 for actin alone to 2.5 in the presence of 2  $\mu\text{M}$  (R/W)16. At 5  $\mu\text{M}$  (R/W)16, fluorescence signal increase was abolished, and a stable plateau was observed instead that corresponded to  $14 \pm 2\%$  (four independent experiments) of the plateau reached by F-actin alone. The same experiments were repeated in the presence of 0.1% (15  $\mu\text{M}$ ) or 1% (150  $\mu\text{M}$ ) bovine serum albumin (Fig. 2B), a protein with an

acidic pI value similar to actin, to decipher how these effects would be influenced by nonspecific conflicting interactions. At substoichiometric concentrations, the peptide did not increase the rate of actin polymerization in the presence of BSA, although the same plateau was reached. Above stoichiometry, at the opposite, reduced fluorescence intensity was always observed with a plateau 2-fold above G-actin fluorescence. A spin-down assay (Fig. 2C) was performed that demonstrates that F-actin was also formed under these conditions and in similar amounts when compared with actin alone and thus that actin polymerization was not inhibited. Differences in pyrene quenching are the molecular basis for the actin-pyrene polymerization assay. Indeed as G-actin structure is slightly modified in the polymer, pyrene is no longer exposed to quenching by adjacent tryptophan or tyrosine amino acids in F-actin. It has been shown that under heavy meromyosin binding, pyrene-labeled F-actin exhibits fluorescence decrease to values intermediate between those of G-actin and of F-actin alone (32). In that study, it was assessed that the binding of meromyosin to F-actin alters the local conformation of each protomer, making it similar (but not identical) to that of G-actin. (R/W)16 could influence in the same way pyrene fluorescence through binding to lower affinity sites. This quenching would not be surprising because it has been shown that pyrene could be quenched by Trp or Arg (33, 34), the two amino acids that compose (R/W)16. The fact that no similar quenching was observed when the peptide was added to preformed F-actin observation could simply indicate a slight conformational change of the protomer upon F-actin formation in the presence of (R/W)16. Alternatively, lower affinity binding sites (occupied above stoichiometry) could lock the structure of G-actin in a conformation that does not prevent actin polymerization but inhibits pyrene fluorescence by local environmental changes of the fluorophore in the protomer.

The inhibited rate increase at substoichiometric peptide concentrations, together with the fluorescence quenching at higher concentrations, in the presence of BSA are only apparently conflicting observations. (RW)16 binds ( $K_d$  value about 20  $\mu\text{M}$ ) competitively to BSA, which has a similar acidic pI value as actin (5.5 versus 5.2, respectively). This binding would make the peptide available at too low concentration for influencing the polymerization kinetic. Nevertheless, the association/dissociation kinetics of the peptide to BSA could still leave the peptide in excess available for the fluorescence quenching or, alternatively, the filament formed in the presence of an excess (RW)16 would simply, because of the conformational variations of the protomer, present a reduced fluorescence.

**Cell Uptake and Cytotoxicity in 3T3 and EF Fibroblasts**—Because (R/W)16, (R/W)9, and R9 had already been reported as cell-penetrating peptides (25, 28, 35), we just examined with (R/W)9 whether the internalization level was similar in 3T3 and

FIGURE 1. NMR and calorimetry analyses of the interaction of actin with (R/W)16 and (R/W)9. A, ITC of the interaction of actin with (R/W)16 (A1) or (R/W)9 (A2). B1, one-dimensional NMR spectrum of free G-actin, free (R/W)9, and (R/W)16; B2, one-dimensional NMR spectrum of G-actin with up to 6 eq of (R/W)16; B3, one-dimensional NMR spectrum of G-actin with up to 5 eq of (R/W)9. The gray bar highlights the zone that is characteristic of protons of tryptophan side chain. C1, NMR spectrum of free thymosin  $\beta$ 4; C2, actin-thymosin  $\beta$ 4 1:1 complex; C3 and C4, actin-thymosin  $\beta$ 4 in the presence of (R/W)16 in a stoichiometry 1:1:0.6 (C3) or 1:1:1 (C4).

## Cell-penetrating Peptide-induced Stress Fiber Formation

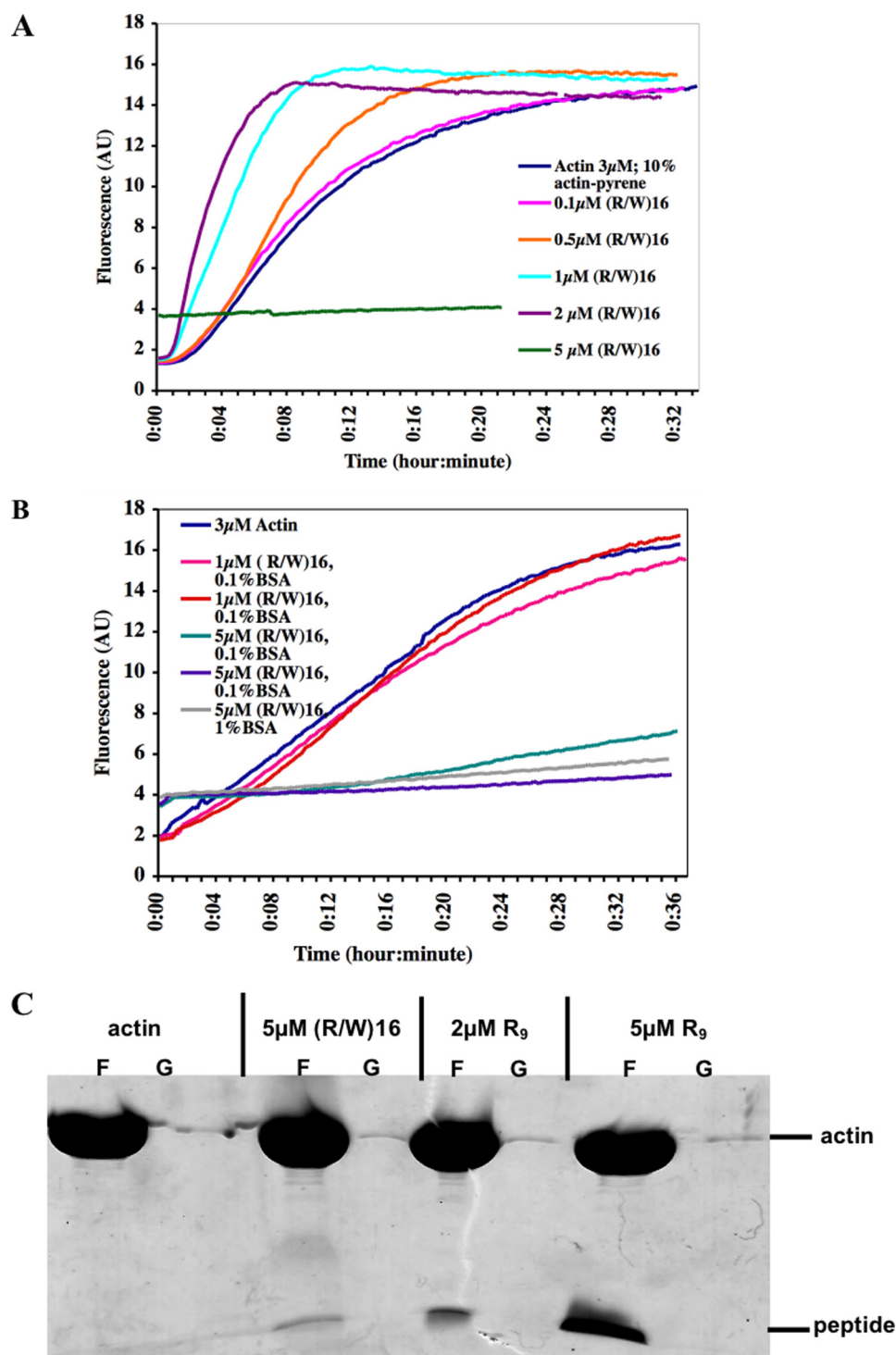


**FIGURE 2. Effect of (R/W)16 on actin-pyrene polymerization.** A, pyrene-labeled and unlabeled actin monomers (3  $\mu$ M) were mixed to obtain 10% pyrene-actin in G buffer. The reaction was started by the addition of 10 $\times$  KMEI (500 mM KCl, 10 mM MgCl<sub>2</sub>, 10 mM EGTA and 100 mM imidazole-HCl, pH 7). Kinetics of polymerization was obtained by measurement of fluorescence signal increase related to actin-pyrene incorporation into actin polymers (22). AU, arbitrary units. B, effect of BSA on (R/W)16 induced actin polymerization and fluorescence signal. C, 10% SDS-PAGE following spin-down assay (75,000 rpm for 30 min) of actin incubated for 30 min with 5  $\mu$ M (R/W)16 in the presence of 0.1% BSA. G, G-actin; F, F-actin.

EF cells as in CHO-K1 cells. Mass spectrometry-based quantification assays (36) were done in parallel in the three cell lines. A similar intracellular quantity was measured in the three cell lines (supplemental Fig. S1); about 10 pmol (about 40  $\mu$ M/cell) of (R/W)9 were measured after a 75-min incubation with

250,000 cells. This value dropped down to 3 pmol (about 10  $\mu$ M/cell) after 18 h, as reported (28).

The effect of the peptides on cell viability or membrane integrity was then measured. Only the (R/W)16 peptide was found toxic and to affect the membrane integrity at concentrations  $\geq 20$   $\mu$ M (supplemental Fig. S1, only cell viability is shown).

(R/W)9, (R/W)16, and R9, but not (D)(R/W)9, Induce a Significant Morphology Reversion of EF Cells toward 3T3 Cell Shape—To get insight into the effect of these peptides in cells, these peptides were tested in NIH-3T3 (3T3) and NIH-3T3-EF (EF) fibroblasts (27). These two cell lines differ markedly in their actin organization (27). 3T3 fibroblasts have a star-flattened shape due to an organized actin filament network with thick stress fibers (Fig. 3). In these cells, zyxin is localized at focal adhesions and cell-to-cell contact points. On the other hand, 3T3 fibroblasts transformed with the EWS-FLI1 oncoprotein exhibit a complete disruption of their actin cytoskeleton, retaining very few stress fibers, focal adhesions, and cell-to-cell contacts (Fig. 3). In addition, zyxin is expressed at very low levels and remains diffusely distributed throughout the cytoplasm (27). Actin is predominantly diffused in the cytosol or bundled in lamellipodia. In addition, EF cells are characterized by a loss of cell-cell contacts, a cell polarization, and an increase in the cell motility. Finally, zyxin is underexpressed in EF cells when compared with 3T3 cells (27).

Peptides were incubated at 10  $\mu$ M for 18–24 h with EF cells before fixation and labeling of actin (phalloidin-fluorescein isothiocyanate), zyxin (monoclonal antibody, secondary antibody-TRITC), and the nuclei (4',6-diamidino-2-phenylindole) before epifluorescence microscopy analysis (Fig. 4). The experiments were reproduced five times independently and always gave the same results. (R/W)16, (R/W)9, and R9 could induce stress fiber reorganization in EF cells (Fig. 3), whereas their potential effect in 3T3 cells was not visible (not shown). In addition, cell-cell contacts were re-established in the presence of

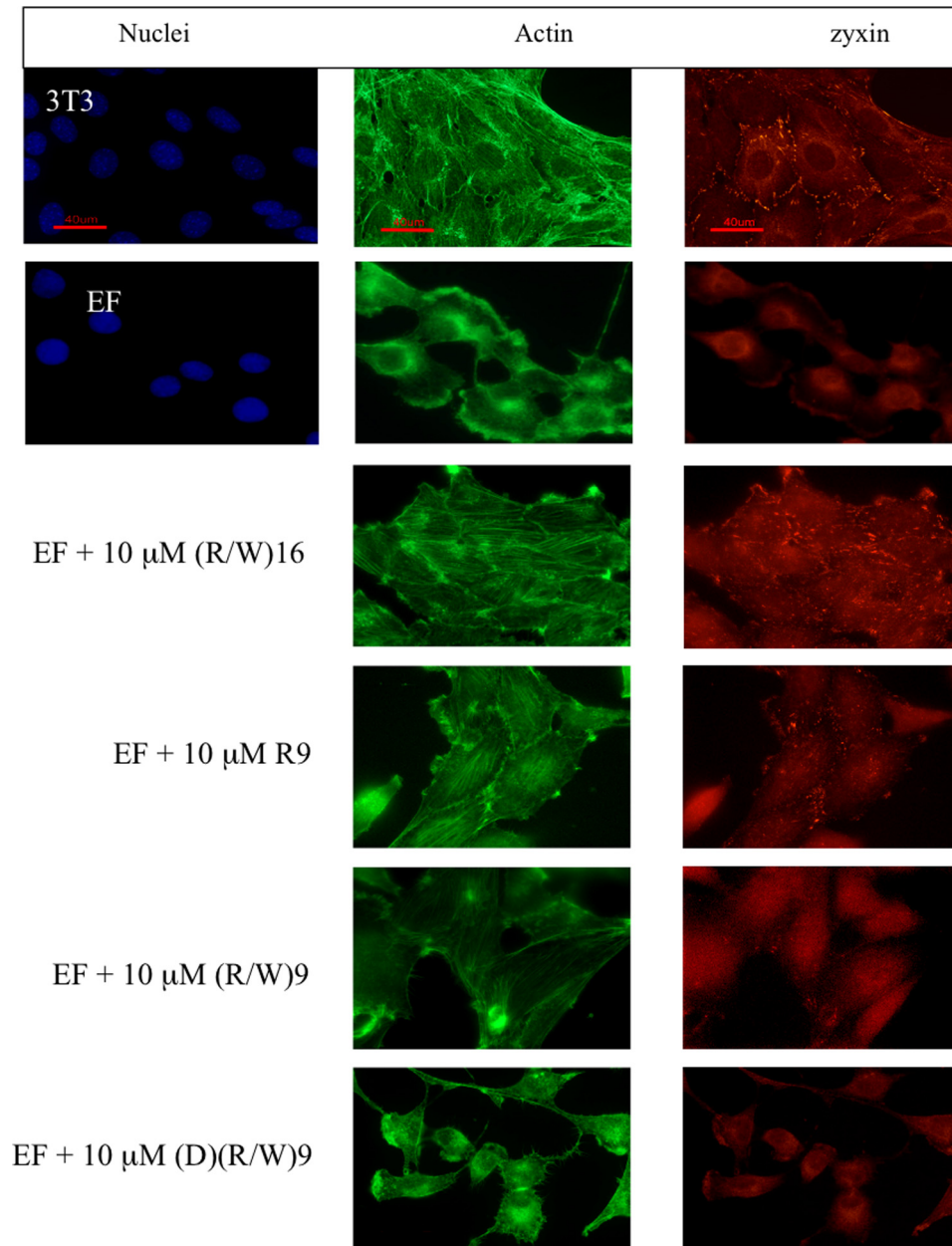


**FIGURE 3. Actin organization and zyxin localization in 3T3 and EF cells.** Shown is fluorescence microscopy (Nikon Eclipse TE2000-S, X60 PlanFluor) observation of actin (green) labeled with phalloidin-fluorescein isothiocyanate. Red, zyxin with a mouse antibody and a secondary donkey anti-mouse IgG antibody conjugated to TRITC. Blue, nuclei labeled with 4',6-diamidino-2-phenylindole. EF cells were incubated for 18–24 h with 10  $\mu\text{M}$  (R/W)16, (R/W)9, R9, and (D)(R/W)9.

these peptides in EF when compared with control 3T3 and EF cells (Fig. 3). The effect of the enantiomeric form of (R/W)9, containing all D-amino acids, was assayed in the same conditions. Although internalized in cells (not shown) without inducing cytotoxicity (supplemental Fig. S1), the D-amino acids containing peptide had no effect on actin organization in 3T3 and EF cells (Fig. 3).

To define in a more quantitative manner the observation of the peptide-induced stress fiber formation made by fluorescence microscopy, different classes of cells according to their morphology were distinguished (Fig. 4). Cells resembling non-tumoral ones, with a star-flattened shape, actin cytoskeleton organized as stress fibers connected to the cell junctions, and

zyxin localization at focal adhesion points, were classified as non-tumoral (*N*) cells. Cells with a rounded shape, actin bundles in lamellipodia, or diffuse actin and zyxin in the cytosol were classified as tumoral (*T*) cells. Remaining cells with an undefined shape with few cell-cell contacts, small stress fibers, and no zyxin specific localization were difficult to grade and described as undetermined (*ND*) cells.

The non-tumoral cells were the major class for 3T3 cells, whereas the tumoral class best defined the EF cells (Fig. 4). After an 18–24-h incubation with 10  $\mu\text{M}$  peptides, the repartition of the cells between the three classes was similar for (R/W)16, (R/W)9, and R9 (Fig. 4). When compared with the tumoral class, the non-tumoral class became major in the EF population incubated with the peptides (Fig. 4). About 35–40% of EF cells were ranked in the undetermined class. Similar results were obtained in the presence of jasplakinolide, although the undetermined class was much less populated than for the cell-penetrating peptides. Similar results were also obtained after a 2-h incubation instead of an 18-h incubation of the EF cells with the peptides. By contrast, the enantiomeric analogue (all D-amino acids) of the (R/W)9 peptide did not have any visible effect in these tumoral cells. Finally, the effects of the peptides (10  $\mu\text{M}$ ) on actin organization in 3T3 cells were not morphologically perceptible (Fig. 4). Therefore, the three peptides were effective (via a chiral recognition) to induce actin stress fibers, cell-cell contacts, and partial

zyxin relocation at focal adhesion points in tumoral EF cells.

**(R/W)16 Reduces the Cell Motility of EF Cells**—An increased motility associated with the absence of actin cytoskeleton organization and actin polymerization has been described for EF cells (27). Therefore, we have studied the evolution of EF cell motility in the presence of the most efficient peptide selected from the previous tests, (R/W)16 (Fig. 5). Cell migration was recorded for 18 h with a numerical camera (one image every 4 min), and cell movements were analyzed with MetaMorph software. Parameters of motility were determined as the distance ( $\mu\text{m}$ ), migration speed ( $\mu\text{m}/\text{min}$ ) (Fig. 5A), and random motility coefficient  $\mu$  ( $\mu\text{m}^2/\text{min}$ ) (Fig. 5B) that reflect the ability of the cell to migrate and colonize a new area (directional persis-

## Cell-penetrating Peptide-induced Stress Fiber Formation

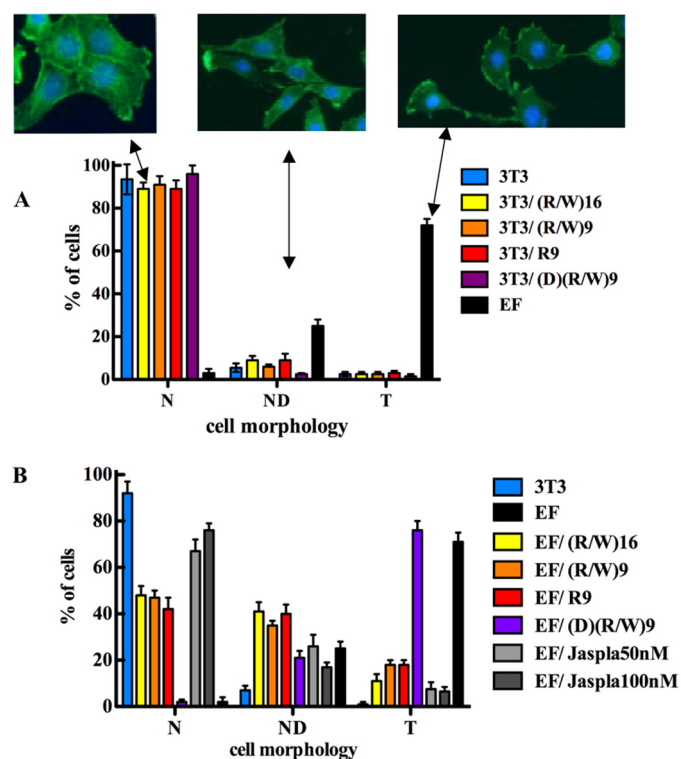


**FIGURE 4. Quantitative analysis of the morphological effects of the cell-penetrating peptides on 3T3 and EF cells.** In three independent experiments, more than 500 3T3- (A) or (B) EF-labeled cells (actin, zyxin, and nucleus) were randomly examined and classified according to morphological parameters (as described under "Results") related to non-tumoral (N), tumoral (T), and undetermined (ND) cells in the absence or in the presence of 10  $\mu\text{M}$  (R/W)16, (R/W)9, R9, (D)/(R/W)9, or 50 and 100 nM jasplakinolide. All conditions were run in parallel. Error bars indicate S.D.

tence). (R/W)16 peptide had no effect on the distance traveled by the cells (not shown). However, (R/W)16 peptide significantly reduced the speed (Fig. 5A) and the random motility coefficient of EF cells (Fig. 5B) to values closer to control 3T3 cells.

*(R/W)16, (R/W)9, and R9 Affect the Ability of EF Cells to Grow with Anchorage Independence*—Cells acquire anchorage-independent growth property during the tumor transformation. This property reflects the capacity of a cell to proliferate without extracellular matrix signaling and can be evaluated by clone formation in semisolid medium. EF malignant and 3T3 non-transformed cells were seeded in culture medium supplemented with methylcellulose in the presence or absence of the three peptides (R/W)9, (R/W)16, and R9 at different concentrations. Peptides were freshly added every third day. After 4 weeks of growth, clones with a diameter larger than 120  $\mu\text{m}$  were counted.

3T3 fibroblasts were unable to grow in semisolid medium, whereas 206 clones of EF fibroblasts could be counted (Fig. 5C). Clone numbers in the different assay conditions were normalized relative to the number of EF cell clones. The percentage of clones decreased by 30% in the presence of 20  $\mu\text{M}$  (R/W)16 peptide (Fig. 5C). (R/W)9 was more effective, and 10  $\mu\text{M}$  led to a significant decrease in the number of clones (25%). An even more pronounced effect was observed in the presence of 10  $\mu\text{M}$  R9 peptide for which the clone number was reduced by 70% ( $p < 0.0001$ ). Therefore, the three cell-penetrating peptides led

to reduction of anchorage-independent growth capacity but with a different rank of efficiency,  $R9 \gg (R/W)9 > (R/W)16$ .

*(R/W)16 Reduces the Migration of EF Cells*—The effect of (R/W)16 was also examined in the wound healing assay. As shown (Fig. 5D), 10  $\mu\text{M}$  (R/W)16 reduced the closure of the wound by EF cells, whereas penetratin (RQIKIWFQNRRMK-WKK), a basic cell-penetrating peptide with the same number of amino acids, could not.

## DISCUSSION

Calorimetry assays show that (R/W)16, (R/W)9, and R9 interact directly with G-actin. The affinities of (R/W)16 and (R/W)9 for G-actin were 0.4 and  $\sim 10 \mu\text{M}$  (and  $\geq 10 \mu\text{M}$  for R9), respectively. A higher apparent affinity and/or higher stoichiometry of (R/W)16 when compared with (R/W)9 was also established from NMR experiments. The reappearance of the signals of (R/W)16 only in samples containing a peptide/actin ratio higher than 6/1 favored a stoichiometry of about five (R/W)16 peptides per actin monomer. NMR data indicate that the peptides (R/W)16 and (R/W)9 also induced either actin oligomerization or aggregation.

The data obtained from a pure actin polymerization assay further support this observation. (R/W)16 increased up to 2.5-fold the rate of actin-pyrene polymerization in a concentration-dependent manner. Above stoichiometric conditions (0.7 excess of (R/W)16), the fluorescence signal stayed at a plateau with a fluorescence intensity about twice the intensity observed with G-actin. This phenomenon could have two origins. First, it could result from the fluorescence quenching of the actin protomers in the filament by the excess of (R/W)16. Alternatively, the protomers in the F-actin formed in the presence of an excess of peptide could present a slight conformational modification, allowing the fluorescence quenching.

The fact that BSA, with a similar acidic pI value as actin (5.5 versus 5.2, respectively), shown to bind (RW)16 with a dissociation constant around 20  $\mu\text{M}$  by ITC measurements (not shown), did reverse the increase of the polymerization rate could be simply due to a reduced concentration of the available peptide. That the fluorescence intensity is at a plateau in excess of peptide could result from competitive binding of the peptide to BSA and polymerizing actin or merely to a global pyrene quenching of actin polymerizing in the presence of excess peptide. Altogether, it demonstrates that the effect of (RW)16 is partially maintained in the presence of binding to other proteins, a situation likely to occur in cells. In this assay, at the opposite, (R/W)9 and R9 did not affect actin polymerization, which might be related to the maximal concentration used (10  $\mu\text{M}$ ) similar to or below their respective affinity for actin.

Preliminary cross-linking data (not shown) and the unbinding of T $\beta$ 4 by (R/W)16, as followed by NMR, further support the hypothesis of a direct interaction with actin and provide some indication of the localization of the interaction site(s). The three peptides were cross-linked to the same actin fragment (Cys<sup>287</sup>-Asp-Ileu-Asp-Ileu-Arg<sup>292</sup>) in subdomain 3 of monomeric actin (barbed end side). This fragment is located on a solvent-exposed loop according to the crystallographic model of Kabsch *et al.* (37). In addition, (R/W)16 was able to compete with the actin-binding protein, thymosin  $\beta$ 4, at a stoichiometry

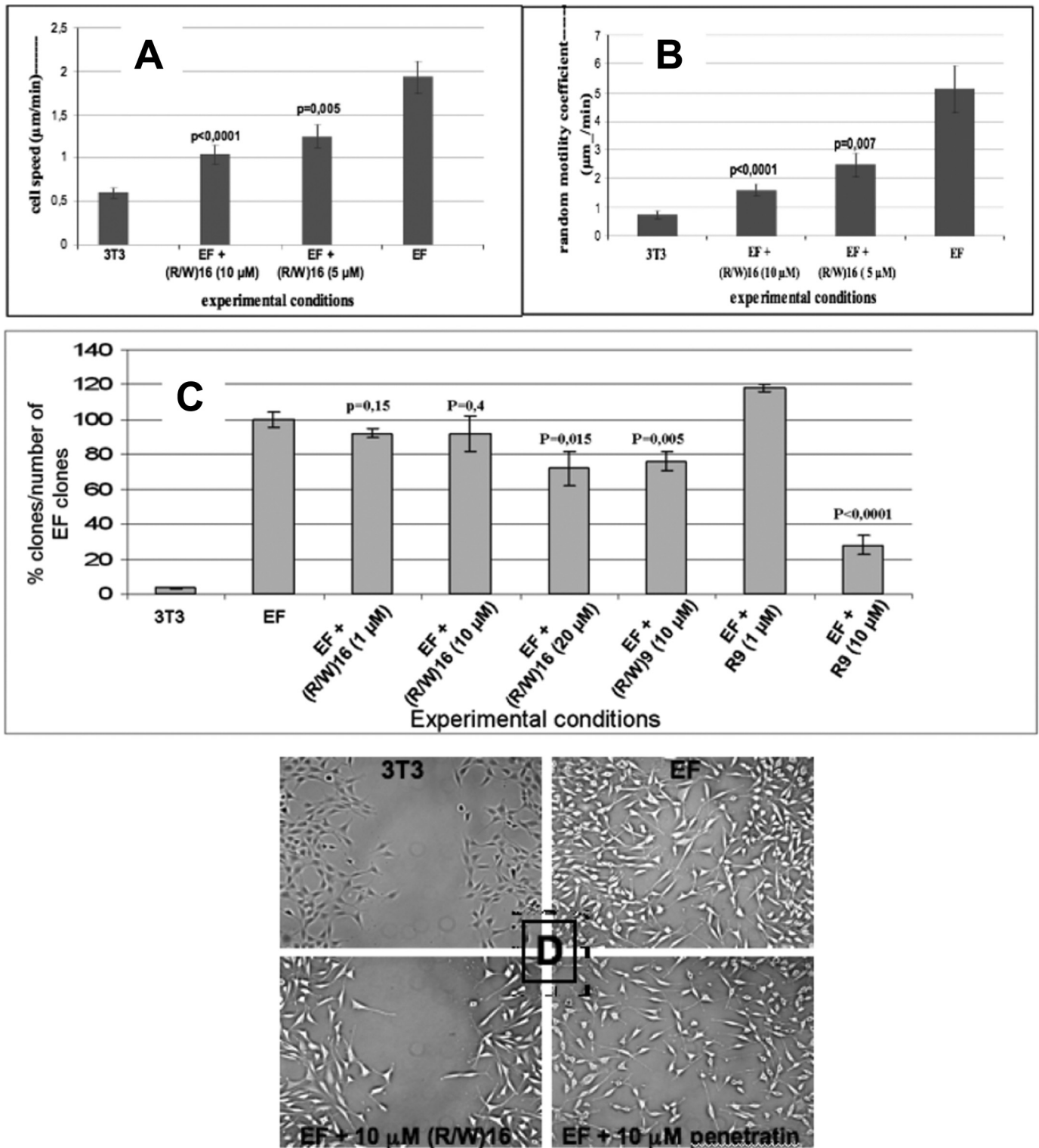


FIGURE 5. Effect of the cell-penetrating peptides on motility, anchorage-independent growth, and migration of EF cells. A and B, effect of (R/W)16 on cell speed (A) and random motility coefficient (B) of EF cells. C, effect of (R/W)16, (R/W)9, and R9 on the capacity of EF cells to grow with anchorage independence. Error bars indicate S.D. D, effect of (R/W)16 and of another cell-penetrating peptide with the same number of amino acids, penetratin, in the wound-healing assay.

of 1:1:1. Thymosin  $\beta_4$  makes extensive interactions with G-actin, in particular with the N terminus residues forming an  $\alpha$  helix buried in the hydrophobic cleft located between subdomains 1 and 3 in actin, a region where Cys-374 (bearing the pyrenyl moiety) is also located. One hypothesis for this phe-

nomenon could be a competitive binding, possibly at this site, an attractive hypothesis in view of the potential of (R/W)16 to fold in an amphipathic helix. In addition, (R/W)16, (R/W)9, and R9 were shown to partially reverse the tumoral phenotype of malignant EF cells (induction of stress fibers and cell-cell-con-

## Cell-penetrating Peptide-induced Stress Fiber Formation

tacts but only partial relocation of zyxin at focal adhesion cell points).

Indeed, in these malignant cells, in the presence of (R/W)16, (R/W)9, and R9, stress fibers and cell-cell contacts could be observed by fluorescence microscopy, whereas these peptides did not have any visible effects on control 3T3 cells. These morphological effects of the cell-penetrating peptides were similar to those observed with jasplakinolide, a molecule well known to induce actin polymerization. This capacity to reorganize actin could also affect the motility of EF cells (migration speed, random motility coefficient, wound healing repair), as demonstrated with (R/W)16. Furthermore, the ability of malignant EF cells to grow in anchorage independence was also reduced in the presence of the three cell-penetrating peptides. However, the peptides might also interact with other proteins, and actin dynamics are finely regulated by actin-binding proteins in cells. Therefore, it is not surprising that the affinity of the peptides for actin *in vitro* and their efficiency on actin dynamics in cells were different. Taking together the high internalization efficiency, the long-lasting (24–48 h) morphological effects of the peptides in cells, and the inactivity of the D-amino acid (R/W)9 analogue (which also internalizes efficiently), these peptides likely exert these effects on intracellular actin and not through recognition of extracellular membrane components such as glycosaminoglycans or integrins that are coupled to intracellular signaling that control actin organization (38–42).

The deficiency of actin organization in stress fibers in EF cells was previously related to underexpression and delocalization of zyxin (27). In addition, it has been reported with zyxin-null fibroblasts that, in addition to actin remodeling deficit, vasodilator-stimulated phosphoprotein (VASP) was mislocalized (43). Finally, it has been established that actin polymerization at focal adhesions strongly depends on mechanical forces in which zyxin is particularly involved (44). Therefore, the effect of the peptides described herein might also be to replace and/or recruit the zyxin-VASP complex required to anchor actin filaments to the cell membrane. Thus, once internalized, the peptides bound to the internal membrane leaflet could recruit and induce actin filament formation. Finally, preliminary *in vivo* assays (not shown) in mice with xenografted tumors show the capacity of (R/W)16 to reduce significantly the tumor growth.

Altogether, the data reported herein shed new light on cell-penetrating peptides, which are potentially biologically active peptides interacting with extracellular (45) or intracellular (this study) protein targets. Therefore, these cell-penetrating peptides might have very interesting biological activities that deserve to be fully studied.

*Acknowledgments*—We thank Drs. Gérard Bolbach and Emmanuelle Sachon from the platform of Mass Spectrometry and Proteomics of UPMC for their help in mass spectrometry analysis and Vanessa Point for assistance in peptide synthesis.

### REFERENCES

1. Joliot, A., Pernelle, C., Deagostini-Bazin, H., and Prochiantz, A. (1991) *Proc. Natl. Acad. Sci. U.S.A.* **88**, 1864–1868
2. Joliot, A. H., Triller, A., Volovitch, M., Pernelle, C., and Prochiantz, A. (1991) *New Biol.* **3**, 1121–1134

3. Derossi, D., Joliot, A. H., Chassaing, G., and Prochiantz, A. (1994) *J. Biol. Chem.* **269**, 10444–11050
4. Hansen, M., Milk, K., and Langel, U. (2008) *Adv. Drug Deliv. Rev.* **60**, 572–579
5. Jiao, C. Y., Delaroché, D., Burlina, F., Alves, I. D., Chassaing, G., and Sagan, S. (2009) *J. Biol. Chem.* **284**, 33957–33965
6. Jones, A. T. (2008) *Int. J. Pharm.* **354**, 34–38
7. Dietz, G. P., and Bähr, M. (2004) *Mol. Cell Neurosci.* **27**, 85–131
8. Turner, J. J., Jones, S., Fabani, M. M., Ivanova, G., Arzumano, A. A., and Gait, M. J. (2007) *Blood Cells Mol. Dis.* **38**, 1–7
9. Sugiyama, S., Prochiantz, A., and Hensch, T. K. (2009) *Dev Growth Differ.* **51**, 369–377
10. Saar, K., and Langel, Ü. (2007) in *Handbook of Cell-Penetrating Peptides* (Langel, Ü., ed) pp. 553–566, CRC Press, Boca Raton, FL
11. Hartwig, J. H., Thelen, M., Rosen, A., Janmey, P. A., Nairn, A. C., and Aderem, A. (1992) *Nature* **356**, 618–622
12. Oriol-Audit, C. (1978) *Eur. J. Biochem.* **87**, 371–376
13. Brown, S. S., and Spudich, J. A. (1979) *J. Cell Biol.* **80**, 499–504
14. Wohnsland, F., Schmitz, A. A., Steinmetz, M. O., Aebi, U., and Vergeres, G. (2000) *Biophys. Chem.* **85**, 169–177
15. Wohnsland, F., Steinmetz, M. O., Aebi, U., and Vergères, G. (2000) *J. Struct. Biol.* **131**, 217–224
16. Tang, J. X., and Janmey, P. A. (1996) *J. Biol. Chem.* **271**, 8556–8563
17. Tang, J. X., Szymanski, P. T., Janmey, P. A., and Tao, T. (1997) *Eur. J. Biochem.* **247**, 432–440
18. Shikina, K., Kwon, H., Kakugo, A., Furukawa, H., Osada, Y., Gong, J. P., Aoyama, Y., Nishioka, H., Jinnai, H., and Okajima, T. (2008) *Biomacromolecules.* **9**, 537–542
19. Chereau, D., Kerff, F., Graceffa, P., Grabarek, Z., Langsetmo, K., and Dominguez, R. (2005) *Proc. Natl. Acad. Sci. U.S.A.* **102**, 16644–16649
20. Renault, L., Bugyi, B., and Carlier, M. F. (2008) *Trends Cell Biol.* **18**, 494–504
21. Paunola, E., Mattila, P. K., and Lappalainen, P. (2002) *FEBS Lett.* **513**, 92–97
22. Hertzog, M., van Heijenoort, C., Didry, D., Gaudier, M., Coutant, J., Gigant, B., Didelot, G., Préat, T., Knossow, M., Guittet, E., and Carlier, M. F. (2004) *Cell* **117**, 611–623
23. Dominguez, R. (2004) *Trends Biochem. Sci.* **29**, 572–578
24. Dominguez, R. (2007) *Ann. N.Y. Acad. Sci.* **1112**, 86–94
25. Derossi, D., Chassaing, G., and Prochiantz, A. (1998) *Trends Cell Biol.* **2**, 84–87
26. Spitz, J. A., Polard, V., Maksimenko, A., Subra, F., Baratti-Elbaz, C., Méallet-Renault, R., Pansu, R. B., Tauc, P., and Auclair, C. (2007) *Anal. Biochem.* **367**, 95–103
27. Amsellem, V., Kryszke, M. H., Hervy, M., Subra, F., Athman, R., Leh, H., Brachet-Ducos, C., and Auclair, C. (2005) *Exp. Cell Res.* **304**, 443–456
28. Delaroché, D., Aussedat, B., Aubry, S., Chassaing, G., Burlina, F., Clodic, G., Bolbach, G., Lavielle, S., and Sagan, S. (2007) *Anal. Chem.* **79**, 1932–1938
29. Domanski, M., Hertzog, M., Coutant, J., Gutsche-Perelroizen, I., Bontems, F., Carlier, M. F., Guittet, E., and van Heijenoort, C. (2004) *J. Biol. Chem.* **279**, 23637–23645
30. Delaglio, F., Grzesiek, S., Vuister, G. W., Zhu, G., Pfeifer, J., and Bax, A. (1995) *J. Biomol. NMR* **6**, 277–293
31. Cooper, J. A., Walker, S. B., and Pollard, T. D. (1983) *J. Muscle Res. Cell Motil.* **4**, 253–262
32. Kouyama, T., and Mihashi, K. (1981) *Eur. J. Biochem.* **114**, 33–38
33. Yang, H., and Bohne, C. (1996) *J. Phys. Chem.* **100**, 14533–14539
34. Encinas, M. V., and Lissi, E. A. (1986) *Photochem. Photobiol.* **44**, 579–585
35. Wender, P. A., Mitchell, D. J., Pattabiraman, K., Pelkey, E. T., Steinman, L., and Rothbard, J. B. (2000) *Proc. Natl. Acad. Sci. U.S.A.* **97**, 13003–13008
36. Burlina, F., Sagan, S., Bolbach, G., and Chassaing, G. (2005) *Angew. Chem. Int. Ed. Engl.* **44**, 4244–4247
37. Kabsch, W., Mannherz, H. G., Suck, D., Pai, E. F., and Holmes, K. C. (1990) *Nature* **347**, 37–44
38. Nakase, I., Niwa, M., Takeuchi, T., Sonomura, K., Kawabata, N., Koike, Y., Takehashi, M., Tanaka, S., Ueda, K., Simpson, J. C., Jones, A. T., Sugiura, Y., and Futaki, S. (2004) *Mol. Ther.* **10**, 1011–1022

## Cell-penetrating Peptide-induced Stress Fiber Formation

39. Capila, I., and Linhardt, R. J. (2002) *Angew. Chem. Int. Ed. Engl.* **41**, 390–412
40. Hari, S. P., McAllister, H., Chuang, W. L., Christ, M. D., and Rabenstein, D. L. (2000) *Biochemistry* **39**, 3763–3773
41. Sroka, T. C., Pennington, M. E., and Cress, A. E. (2006) *Carcinogenesis* **27**, 1748–1757
42. Lanzetti, L., Di Fiore, P. P., and Scita, G. (2001) *Exp. Cell Res.* **271**, 45–56
43. Hoffman, L. M., Jensen, C. C., Kloeker, S., Wang, C. L., Yoshigi, M., and Beckerle, M. C. (2006) *J. Cell Biol.* **172**, 771–782
44. Hirata, H., Tatsumi, H., and Sokabe, M. (2008) *J. Cell Sci.* **121**, 2795–2804
45. Fotin-Mleczek, M., Welte, S., Mader, O., Duchardt, F., Fischer, R., Hufnagel, H., Scheurich, P., and Brock, R. (2005) *J. Cell Sci.* **118**, 3339–3351
46. Goddard, T. D., and Kneller, D. G. (2007) *SPARKY 3*, University of California, San Francisco, CA

## Cell-penetrating Peptides with Intracellular Actin-remodeling Activity in Malignant Fibroblasts

Diane Delaroche, François-Xavier Cantrelle, Frédéric Subra, Carine Van Heijenoort, Eric Guittet, Chen-Yu Jiao, Laurent Blanchoin, Gérard Chassaing, Solange Lavielle, Christian Auclair and Sandrine Sagan

*J. Biol. Chem.* 2010, 285:7712-7721.

doi: 10.1074/jbc.M109.045872 originally published online December 27, 2009

---

Access the most updated version of this article at doi: [10.1074/jbc.M109.045872](https://doi.org/10.1074/jbc.M109.045872)

### Alerts:

- [When this article is cited](#)
- [When a correction for this article is posted](#)

[Click here](#) to choose from all of JBC's e-mail alerts

### Supplemental material:

<http://www.jbc.org/content/suppl/2009/12/27/M109.045872.DC1>

This article cites 44 references, 11 of which can be accessed free at <http://www.jbc.org/content/285/10/7712.full.html#ref-list-1>